Supplemental Text

Noise analysis of double-barreled ClC channels

For channels with only a single conducting level, the current variance (σ^2) is a function of the mean current amplitude (I), the unitary current amplitude (i) and the number of channels (N)[1;2]:

$$\sigma^2 = iI - \frac{I^2}{N} \tag{1}$$

To develop variance vs. mean current relationships for a double-barreled ClC channel, we used a 6-state-model with two different open states and four closed states[3]. Three states are non-conducting because of a closed common gate. A fourth closed state is characterized by both fast gates closed. There are two conducting states, one with both fast gates open and another one with one fast gate open and the other one closed. This model allows calculation of the probability of the channel being in the closed conformation (P_{closed}) or with one (P_1) or two protopores in the open state (P_2) from the open probabilities of the fast (P_f) and the slow gates (P_s):

$$P_1 = 2P_f P_s (1 - P_f) \tag{2}$$

$$P_2 = P_f^2 P_s \tag{3}$$

$$P_{closed} = 1 - P_1 - P_2 \tag{4}$$

Using these values, mean values (<i>) and variances (σ^2) of the current can be calculated[2]:

$$\langle i \rangle = iP_1 + 2iP_2 = 2iP_f P_s \tag{5}$$

$$\begin{aligned}
\sigma^2 &= NP_{closed}(0 - \langle i \rangle)^2 + NP_1(i - \langle i \rangle)^2 + NP_2(2i - \langle i \rangle)^2 \\
&= N((1 - P_1 - P_2)(0 - iP_1 - 2iP_2)^2 + P_1(i - iP_1 - 2iP_2)^2 + P_2(2i - iP_1 - 2iP_2)^2) \\
&= N \cdot 2i^2 \cdot P_f P_s \cdot (1 - 2P_f P_s + P_f)
\end{aligned} \tag{6}$$

This calculation predicts that a plot of the variance versus the mean current amplitude does not always result in a parabolic distribution for double-barreled channels. Upon voltage steps that change fast and slow gate open probabilities in opposite directions (Figures 1 and 2), a loop-like variance vs. mean current plot is expected (see Figure 3 and supplemental Figure 2). Since

$$I \; = N \cdot i \cdot P_1 + N \cdot 2i \cdot P_2 = 2Ni \cdot P_f P_s \tag{7}$$

equation (6) can be converted into

$$\sigma^2 = (i + iP_f) \cdot I - \frac{I^2}{N} \tag{8}$$

Simulated variance vs. mean current relationships for ClC-K-type chloride channels

We next simulated variance vs. mean current relationships for double-barreled channels under several conditions. Supplemental Figure 2 A gives variance vs. mean current plots (equation 8) for a change of slow gate open probability from 1 to 0. When P_f is fixed in the open state ($P_f = 1$), the plot displays a parabola with a slope at zero current ($I = 0$) that corresponds to the current amplitude of a single channel with two open protopores (blue line in supplemental Figure 2 A). In case of a constantly open slow gate ($P_s = 1$) and a time-dependent change in the fast gate open probability from $P_{f,0} = 0$ to $P_{f,\infty} = 1$, the slope of the calculated parabola at zero current corresponds to the protopore unitary current amplitude (red line in supplemental Figure 2 A). Black lines in supplemental Figure 2 A show simulations for channels whose open probability of the slow gate changes from $P_{s,0} = 1$ to $P_{s,\infty} = 0$ ($\tau_{slow} = 50$ ms) and the fast gate open probability from $P_{f,0} = 0$ to varying steady state values $P_{f,\infty}$ between 0.25 and 1 ($\tau_{fast} = 5$ ms). In these simulations, the current amplitude initially increases due to the fast activation process and then slowly decreases due to deactivation of the common gate. During

fast gate activation at high P_s the channel will be predominantly in a state with a single open protopore, whereas during deactivation an increased P_f and a low P_s results in a higher probability of finding both protopores open. The transition from a single pore conductance to a double pore conductance augments the variance with increasing P_f. Noise analysis therefore displays two different variance values for the same current amplitude, one obtained during activation and the other obtained during deactivation. The lower variance will be found in the rising phase of the current and the higher variance in the decaying phase.

Supplemental Figure 2 B shows a comparison of simulated values (black line) with experimental data (grey symbols). In this example the macroscopic current of mutant V166E rClC-K1 channels in the absence of barttin is analyzed for a voltage step from -180 mV to +145 mV. The parameters i, P_f, P_s, τ_{fast} and τ_{slow} were obtained from the experimental data of this study and the number of channels N was adjusted to match the macroscopic current amplitude. Using the same values, but considering the fast gate as a common gate and two slow gates as independent protopore gates results in a distinct variance vs. mean current plot (supplemental Figure 2 C). In this case the variance during fast activation is larger than the variance during slow deactivation. We conclude that the common gate in ClC-K channels is the slow gate and the individual protopores are gated by two independent fast gates.

REFERENCES

1. Sigworth FJ: The variance of sodium current fluctuations at the node of Ranvier. *J Physiol (London)* 307: 97-129, 1980

2. Alvarez O, Gonzalez C, Latorre R: Counting channels: a tutorial guide on ion channel fluctuation analysis. *Adv Physiol Educ* 26: 327-341, 2002

3. Accardi A, Pusch M: Fast and slow gating relaxations in the muscle chloride channel CLC-1. *J Gen Physiol* 116: 433-444, 2000

Supplemental Figure 1. Single-channel recordings from rat ClC-K1 without barttin. (A-C; F-H) Single-channel recordings from excised inside-out patches containing WT (A-C) or V166E (F-H) rClC-K1. Portions of the recordings in (A) and (F) that are shown on an expanded time scale in (B-C) and (G-H) are indicated (a-d). (D-E; I-J) Amplitude histograms of the registrations shown in (A-C) (WT rClC-K1) or (F-H) (V166E rClC-K1).

Supplemental Figure 2. Simulated variance vs. mean current relationships for ClC-K-type chloride channels. (A) Calculated variance vs. mean current relationships, with the fast gate fixed in the open state ($P_f = 1$) and P_s changing from 1 to 0 (initial slope = 2i) (blue parabola) or with the slow gate fixed in an open state ($P_s = 1$) and P_f changing from 0 to 1 (initial slope = i) (red parabola). Black lines give simulations for P_s changing from 1 to 0 and P_f from 0 to varying steady state values as indicated ($P_{f,\infty}$). (B and C) Comparison of experimental data of V166E rClC-K1 channels in the absence of barttin (grey symbols) with calculated values (black line) simulating the slow (B) or the fast (C) process as common gating of the double-barreled channel (blue and red lines correspond to simulations shown in A).

Supplemental Figure 3. Single-channel recordings from rat ClC-K1/barttin. (A and D) Single-channel recordings from an excised inside-out patch containing WT rClC-K1/barttin held at +45 mV (A) or -55mV (D). (B and E) Amplitude histograms of the registrations shown in A and D. (C and F) Probabilities of the three current levels, closed, open 1 and open 2 at +45 mV (C) and -55 mV (F). The measured state probabilities are represented by bars, whereas the symbols denote the predicted binomial distribution of state probabilities calculated from $P_o = 6.5\%$ in (C) and $P_o = 7.3\%$ in (F) of two independently gated protopores.

WT rClC-K1

A +50 mV
a
b
-50 mV
c
d
2 pA
5 s

B -50 mV
c 0
.... 1
d 0
2 pA 1
100 ms

C +50 mV
a 1
.... 0
b 1
2 pA 0
100 ms

D -50 mV

E +50 mV

V166E rClC-K1

F 0 mV
+95 mV
+95 mV
-105 mV
-105 mV
a
c
2 pA
b
d
10 s

G -105 mV
a 0
.... 1
.... 2
c 0
.... 1
2 pA 2
500 ms

H +95 mV
b 1
.... 0
d 1
2 pA 0
500 ms

I -105 mV

J +95 mV
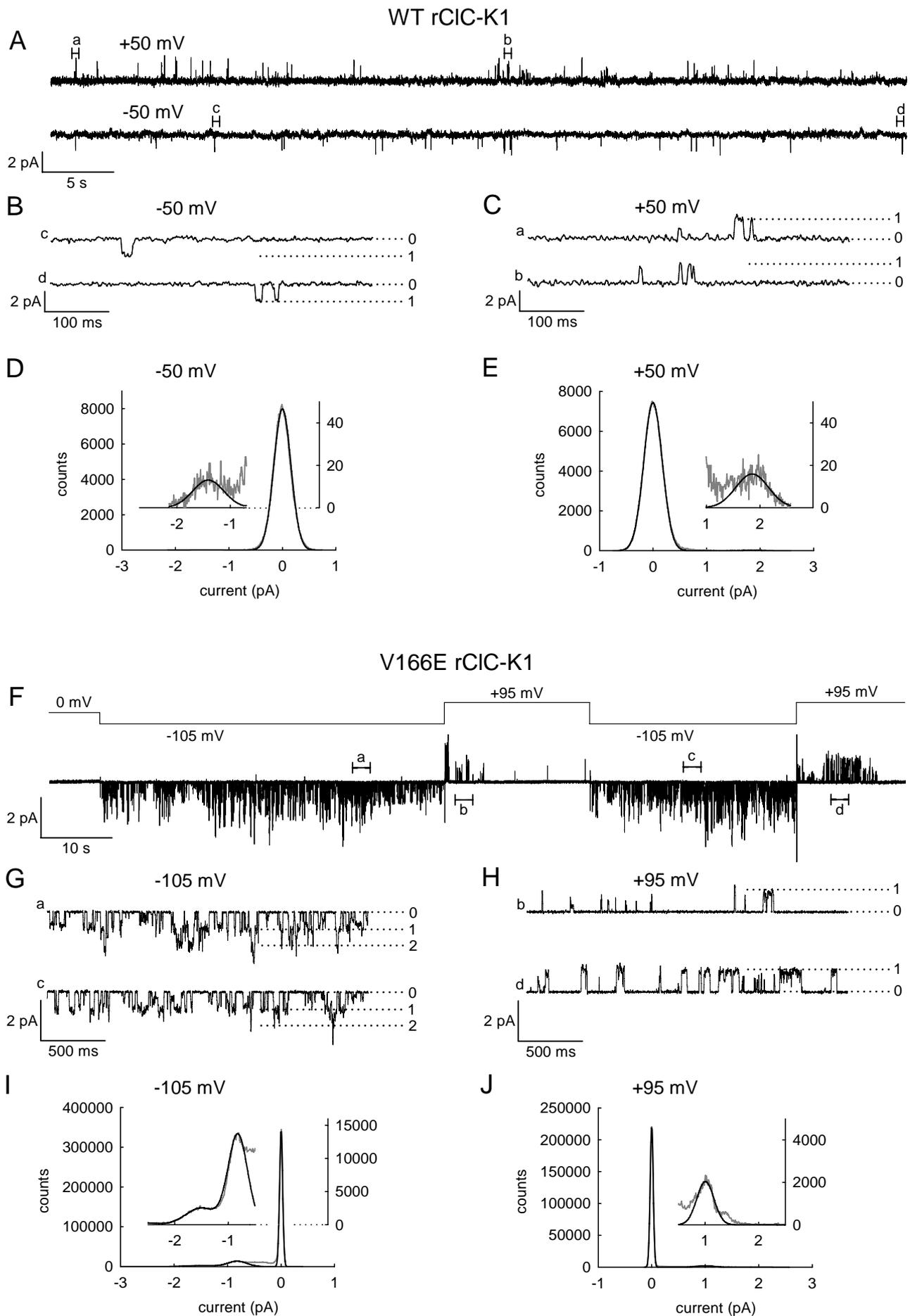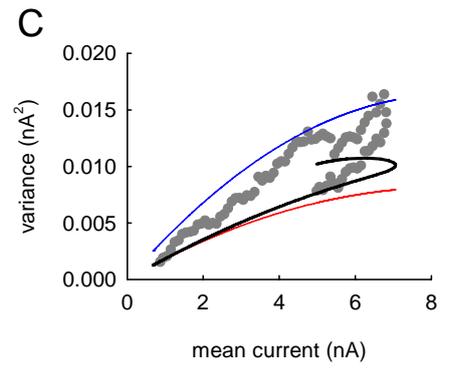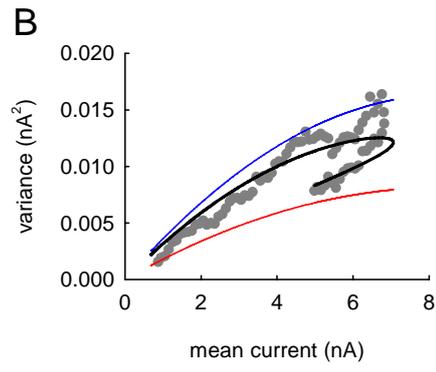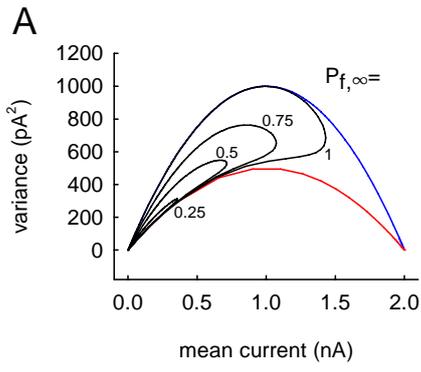
suppl. Fig. 1

suppl. Fig. 2

WT rClC-K1/barttin

suppl. Fig. 3